J Mater Sci (2006) 41:5739–5742
DOI 10.1007/s10853-006-0102-z

LETTER

Fractal geometry of fracture surfaces of a duplex stainless steel

O. A. Hilders · M. Ramos · N. D. Peña · L. Sàenz

Received: 20 October 2004 / Accepted: 28 September 2005 / Published online: 13 May 2006

It is well-known that the micromechanisms of fracture affect the fracture resistance, leaving characteristic information to be collected from the fracture surface. Such qualitative information may be useful in failure interpretation and prevention. On the other hand, since fracture surfaces are irregular microstructures, a prediction of mechanical properties cannot be made by quantitative measurements of fracture features because of the difficulty in arriving at a numerical characterization of the structure. Nevertheless, since Mandelbrot [1] classified the fracture surfaces of metals as approximately fractal, quantitative characterization of their morphological features has rapidly started to be applied in research through a parameter called fractal dimension D, a descriptor of the surface tortuosity with which material properties can be correlated [2–8]. Most investigators have found that the fracture profiles does have a fractal character [9–12] and can be characterized by their linear fractal dimension D_L, which has a non-integer value between 1 and 2.

O. A. Hilders · M. Ramos
School of Metallurgical Engineering and Materials Science, Central University of Venezuela, Apartado 47514, Caracas 1041-A, Venezuela

N. D. Peña
Department of Materials Technology, Federico Rivero Palacios, University of Technology Institute, Apartado 40347, Caracas, 1040-A, Venezuela

L. Sàenz
Department of Materials and Fabrication Processes, University of Carabobo, Apartado 3155, Valencia 2002, Venezuela

O. A. Hilders (✉)
Oswaldo hilders # 5485, Poba international #100, PO Box 02-5255, Miami, FL 33102-5255, USA
e-mail: ohilders@hotmail.com

This research will address the study of two examples of how the fractal geometry enables the quantitative characterization of fracture surfaces, helping to develop potential useful relations between D_L, mechanical properties and fracture surface features. The material studied here is an austenoferritic duplex stainless steel SAF 2205 whose chemical composition, as provided by the supplier, was 22Cr–5.3Ni–3.2Mo–0.17N–0.02C–0.12Si–0.91Mn–0.02P–0.018S–Fe (wt%). Duplex stainless steel are known for their corrosion resistance coupled with excellent tensile, fatigue, and impact strengths [13]. Despite its good performance, one drawback of duplex stainless steels is the susceptibility of the ferrite phase to the so called 475 °C-embrittlement which impairs the thoughness because of the precipitation of a Cr-rich α' phase [14]. In the present study we investigate the relation between the impact toughness and the linear fractal dimensional increment of the corresponding fracture surfaces, as well as the relation between the dimple size and the linear fractal dimensional increment of the fracture surfaces developed in tension, both after aging treatments at 475 °C. The linear fractal dimensional increment is defined by $D_L - 1$. For impact and tension fracture surfaces, the corresponding linear fractal dimensional increments are $(D_L - 1)_{\mathrm{I}}$ and $(D_L - 1)_{\mathrm{T}}$, respectively.

In the as-received condition, the thermal treatments were adjusted such that the microstructure was about 50% α and γ (Fig. 1). This results in optimum strength, formability and weldability [15]. The material was obtained in the form of 31 mm diameter hot rolled rod. ASTM Standard V-notched Charpy impact test samples were prepared with the largest part parallel to the rolling direction, solution treated for 2 h at 1120 °C, water quenched and aged at 475 °C for 1, 2, 6.5, 12, 24, 40 and 120 h. Impact toughness was determined at room temperature as outlined in ASTM E 23–86 [16]. Uniaxial tensile testing was carried

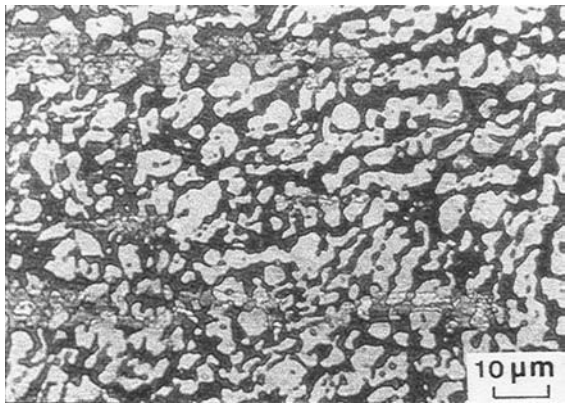

Fig. 1 Optical micrograph of the as-received duplex stainless steel microstructure (dark: ferrite, light: austenite)

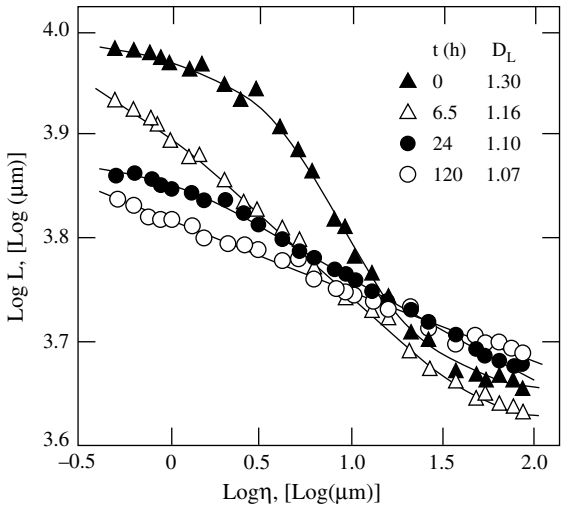

Fig. 2 Richardson–Mandelbrot plots for the impact samples corresponding to the as-received condition (0 h) and aged at 475 °C for 6.5, 24 and 120 h

out at room temperature using cylindrical samples for the same experimental conditions, as explained elsewhere [17]. The fracture surfaces of both, impact and tension samples, were analyzed using a scanning electron microscope operated at 25 kv. In the case of tension fracture surfaces, several fractographs were studied covering at list 1200 dimples for each condition, whose average size was calculated according to the method quoted by Thompson [18]. For impact tests, one broken Charpy sample was selected in each case for fractal evaluation based on the value of the absorbed energy. The sample with toughness value closest to the average was chosen.

Fractal measurements were performed for impact and tension fracture surfaces using the vertical section method, based on the Richardson–Mandelbrot relation [19]:

$$L(\eta) = L_o \eta^{-(D_L - 1)} \tag{1}$$

where L is the apparent length of the fracture profile evaluated with a digitizing software, L_o is a constant and η is the yardstick. From Eq. 1 it follows that $D_L - 1$ can be evaluated from the slope of log L vs. log η:

$$D_L - 1 = -d \log L(\eta)/d \log \eta \tag{2}$$

Figure 2 shows the Richardson–Mandelbrot type curves for the impact samples corresponding to the as-received (0 h) condition, 6.5, 24, and 120 h of aging at 475 °C. The fractal dimensional increment was obtained from the linear portion of the curves, using a least-square fitting method. A similar sets of curves for tension samples of the material under study have been given in a previous paper [4].

Although the fractal dimensional increment for impact and tension fracture surfaces decreases as the time of aging increases (Fig. 3), $(D_L - 1)_I$ remains always higher than $(D_L - 1)_T$, except for 24 h of aging where $(D_L - 1)_I = (D_L - 1)_T = 0.10$. For broken impact samples, little work is expended in the formation of the fractured surfaces as compared to the work dissipated by plastic deformation within the plastic zone of the crack as it grows through the material. In despite of this fact, the work done in forming the impact fracture surfaces is enough to generate a relatively high value of $(D_L - 1)_I$. For tension fracture surfaces the expenditure of work in forming a void sheet is higher than the work dissipated in the plastic zone, but the roughness of the surfaces generated by the dimples is relatively small and so $(D_L - 1)_T$. These effects can be explained as follows: in the impact samples, deep microvoids were observed covering the fracture surfaces for the as-received condition and in the material aged for 1, 2 and 6.5 h. A mixture of dimpled and quasicleavage fracture were observed for 12, 24 and 40 h of aging and finally, for 120 h of aging a complete quasicleavage pattern of fracture was

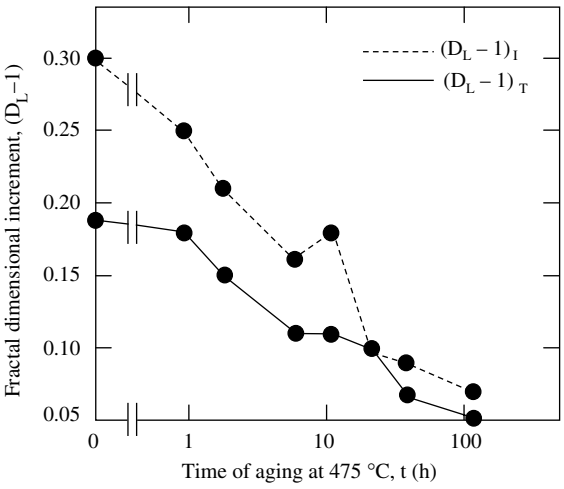

Fig. 3 Effect of aging time at 475 °C on the fractal dimensional increment for impact and tension fracture surfaces

developed. In general, all these fracture morphologies are rougher than the corresponding to the broken tension samples, for which shallow dimples covered between 90% and 100% of the total fractured surface for each tested condition. Some examples of the fracture morphologies developed for tension and impact samples are shown in Fig. 4.

Table 1 shows that the lower the $(D_L - 1)_I$ and $(D_L - 1)_T$ the lower the impact energy and dimple size, respectively. These effects are expected, since when the toughness decreases the work available to the formation of the impact fracture surfaces decreases, and so the fracture surface roughness. On the other hand, as the dimple size decreases, the tension fracture surface roughness decreases and the fractal dimensional increment as well. The relationship between the impact energy E (Ln E) and $(D_L - 1)_I$ is shown in Fig. 5. It can be seen that aging at 475 °C induced significant embrittlement, which promotes a decrease in toughness and fracture surface roughness. These effects are attributed to the precipitation of α', which enhances the tendency to twinning, imposing restrictions on the slip processes and increasing the possibility for microcrack initiation [20]. From Fig. 5 the impact toughness of the austenoferritic alloy can be described by a law of the type developed by Hsiung and Chou [21]:

$$E = 83.10e^{4.52(D_L-1)_I} \quad (3)$$

where 83.10 J represents the impact toughness in Euclidean space (E_0), and 4.52 = dLn $E/d(D_L - 1)_I$. On the other hand, as shown in Fig. 6, an increase in aging time promotes a reduction of the average dimple size and fracture surface roughness for the samples broken in tension. For the average dimple size d_T, we have:

$$d_T = 5.47e^{4.10(D_L-1)_T} \quad (4)$$

where 5.47 μm represents the average dimple size in Euclidean space (d_{T_o}), and 4.10 = dLn $d_T/d(D_L - 1)_T$.

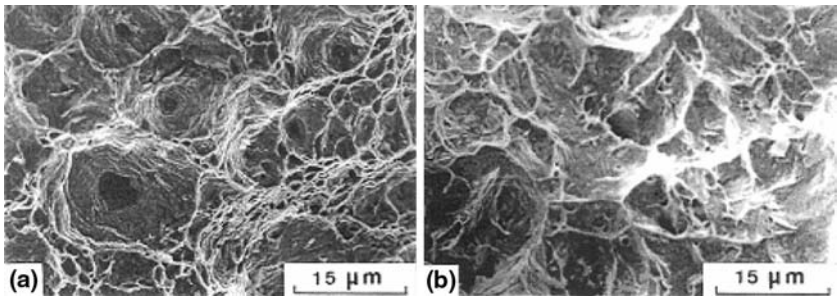

Fig. 4 Fractographs corresponding to some samples aged at 475 °C for 24 h. (**a**) Tension, (**b**) Impact

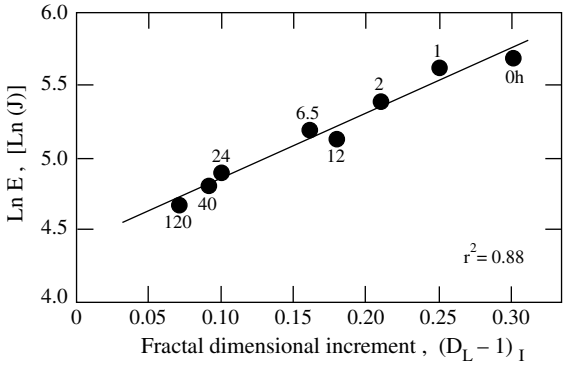

Fig. 5 Dependence of toughness on the impact fractal dimensional increment

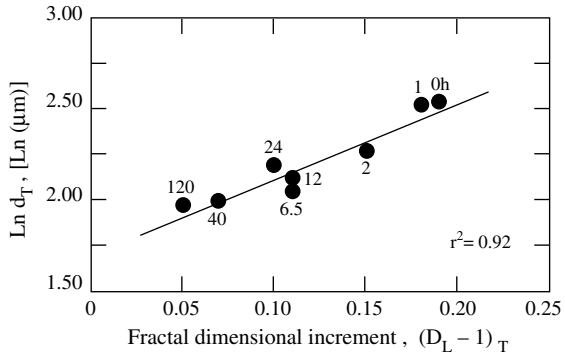

Fig. 6 Dependence of the average dimple size on the tension fractal dimensional increment

Table 1 Toughness dimple size and fractal dimensional increments

Time of aging (h)	Impact Toughness (J)	$(D_L - 1)_I$	Dimple size (μm)	$(D_L - 1)_T$
0	296.4	0.30	12.74	0.19
1	275.2	0.25	12.60	0.18
2	223.6	0.21	9.73	0.15
6.5	181.9	0.16	7.77	0.11
12	170.5	0.18	8.37	0.11
24	135.1	0.10	9.03	0.10
40	122.0	0.09	7.39	0.07
120	108.2	0.07	7.21	0.05

The data reported above bring us closer to a quantitative description of the fracture surfaces through the correlation of fracture morphology or impact toughness with the corresponding fractal dimensional increment. Particularly, since engineering properties often are controlled by microscopic fracture events, it seems to be reazonable that the fractal dimensional increment, which is a measure of the fracture surface roughness, can be related to the crack branching induced changes in impact toughness.

References

1. Mandelbrot BB (1982) The fractal geometry of nature. Freeman, New York, p 109
2. Milman VY, Stelmashenko NA, Blumenfield R (1994) Prog Mater Sci 38:425
3. Li XW, Tian JF, Han NL, Kang Y, Wang ZG (1996) Mater Lett 29:235
4. Hilders OA, Sáenz L, Ramos M, Peña ND (1999) J Mater Eng Perf 8:87
5. Gang JX (1992) J Mater Sci Lett 11:1379
6. Tanaka M, Kato R, Kayama A (2002) J Mater Sci 37:3945
7. Hilders OA, Pilo D (1997) Mater Charact 38:121
8. Mecholsky JJ, West JK, Passoja DE (2002) Phil Mag A 82:3163
9. Mandelbrot BB, Passoja DE, Paullay AJ (1984) Nature 308:721
10. Xie H, Sanderson DJ (1995) Eng Fract Mech 50:529
11. Hilders OA, Peña ND, Ramos M, Sáenz L, Berrío L, Caballero RA, Quintero A (2002) Mater Sci Forum 396–402:1411
12. Stach S, Roskosz S, Cybo J, Cwajna J (2003) Mater Charact 51:87
13. Rajanna K, Pathiraj B, Kolster BH (1997) J Mater Eng Perf 6:35
14. Horvath W, Tabernig B, Werner E, Uggowitzer P (1997). Acta Mater 45:1645
15. Schlapfer HW, Weber J (1986) Mater Tech 2:60
16. ASTM Book of Standards E 23–86 (1989) vol. 3.01, ASTM, Philadelphia, p 198
17. Hilders OA, Sáenz L, Peña N, Ramos M, Quintero A, Caballero RA, Berrío L (2000) Microsc Microan 6(Supp. 2):766
18. Thompson AW (1983) Acta Metall 31:1517
19. Mu ZQ, Lung CW, Kang Y, Long QY (1993) Phys Rev B 48:7679
20. Nyström M, Karlsson B, Wasén J (1990) In: Nordberg H, Fernheden K (eds) Nordic symposium on mechanical properties of stainless steels, Sigtuna, Sweden, October, Avesta Research Foundation, Stockholm, p 70
21. Hsiung JC, Chou YT (1998) J Mater Sci 33:2949